JACS
JOURNAL OF THE AMERICAN CHEMICAL SOCIETY
Article
pubs.acs.org/JACS

π-Electron Conjugation in Two Dimensions

Rico Gutzler*,† and Dmitrii F. Perepichka*,‡

†Max Planck Institute for Solid State Research, Heisenbergstrasse 1, 70569 Stuttgart, Germany

‡Department of Chemistry and Centre for Self-Assembled Chemical Structures, McGill University, Montreal, Quebec H3A 0B8, Canada

Supporting Information

ABSTRACT: Organic oligomers and polymers with extended π-conjugation are the fundamental building blocks of organic electronic devices. Novel routes are being explored to create tailor-made organic materials, and recent progress in organic chemistry and surface chemistry has led to the synthesis of planar 2D polymers. Here we show how extending π-conjugation in the second dimension leads to novel materials with HOMO−LUMO gaps smaller than in 1D polymers built from the same parent molecular repeat unit. Density functional theory calculations on *experimentally realized* 2D polymers grant insight into HOMO−LUMO gap contraction with increasing oligomer size and show fundamental differences between 1D and 2D "band gap engineering". We discuss how the effects of cross-conjugation and dihedral twists affect the electronic gaps.

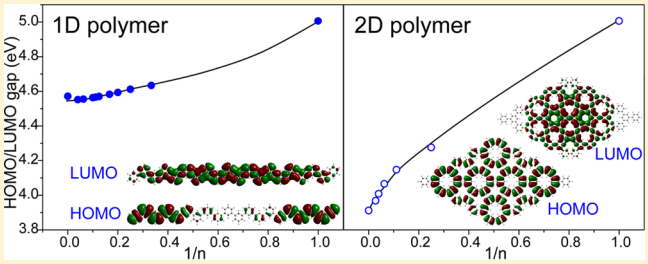

INTRODUCTION

Since the discovery of conductivity in doped polyacetylene (**1.1**),[1] π-conjugated polymers find diverse applications as semiconducting and luminescent materials in electronic and optoelectronic devices,[2,3] sensing,[4,5] and bioimaging.[6] One-dimensional (1D) conjugated polymers and structurally related carbon nanotubes are dominating the field of carbon-based electronics, although two-dimensional (2D) π-functional materials such as graphene (**1.2**) are becoming of increasing importance.[7] Many of the unique properties of graphene are attributed to 2D electron confinement effects. One of the disadvantages of graphene is its vanishing band gap, while a finite gap is desirable for most electronic device applications. This zero gap between valence and conduction band in graphene can be opened by functionalization[8] or by reducing one of its dimensions to create nanoribbons,[9] although this generally results in suppressing charge mobility and other functional properties.

In conjugated 1D polymers, band gap engineering is a mature research area[10−12] that led to a number of new functional organic materials and break-through device properties (e.g., in polymer solar cells[13]). A number of studies have reported the dependence of the HOMO−LUMO gap (HLG) on 1D oligomer length, both experimentally[14] as well as theoretically.[15−17] The HLG of conjugated polymers is commonly tuned by the choice of the molecular repeat unit (its HLG, connectivity, aromaticity), side-chain substituents (affecting the torsional angles), and by alternating donor and acceptor units in the chain.[11] One could expect that similar approaches can be used to control the band gap in two-dimensional π-conjugated systems, but so far, this field remains largely unexplored. Achieving effective conjugation through a molecular building block in several directions (omniconjugation) is rare.[18]

The first theoretical predictions of the properties of 2D conjugated polymers are dated to the 1980s−1990s,[19−21] although the discovery of graphene has spawned an increasing theoretical interest in other 2D carbon allotropes such as porous graphene,[22] graphyne,[20,23−25] graphdiyne,[20,25,26] and related structures.[19−21,25,27−31] Many of these calculated structures (other than graphene) do not have synthetically feasible equivalents in the "real world", although there are exceptions such as porous graphene (**2.2**) recently realized by the Fasel and Müllen groups.[32]

At the same time, the experimental interest in 2D π-conjugated polymers is rapidly growing,[33−38] initiated by the first demonstration in 2007 by Grill, Hecht, and coworkers.[39] Major synthetic progress was made using surface-confined polymerization under ultrahigh vacuum,[32,39−43] but solution-based approaches are also actively explored.[44−46] Alternative routes toward 2D polymers which do not depend on a supporting substrate include photopolymerization of layered single crystals[47] and bulk covalent organic framework (COF) synthesis.[48−50]

Although a growing number of 2D polymers is being synthesized, little is known about their properties and experimental studies remain a huge challenge.[51] The concept of band gap engineering in 2D is especially interesting as the number of intermolecular connections rises faster in 2D than in 1D, which should lead to a different HLG for otherwise similar polymers. This point is addressed here in detail by density functional theory (DFT) calculations for the experimentally

Received: August 12, 2013
Published: September 19, 2013

   dx.doi.org/10.1021/ja408355p | J. Am. Chem. Soc. 2013, 135, 16585−16594

Scheme 1. Chemical Structures of the Calculated 1D (1.1−9.1) and 2D (1.2−9.2) Polymers

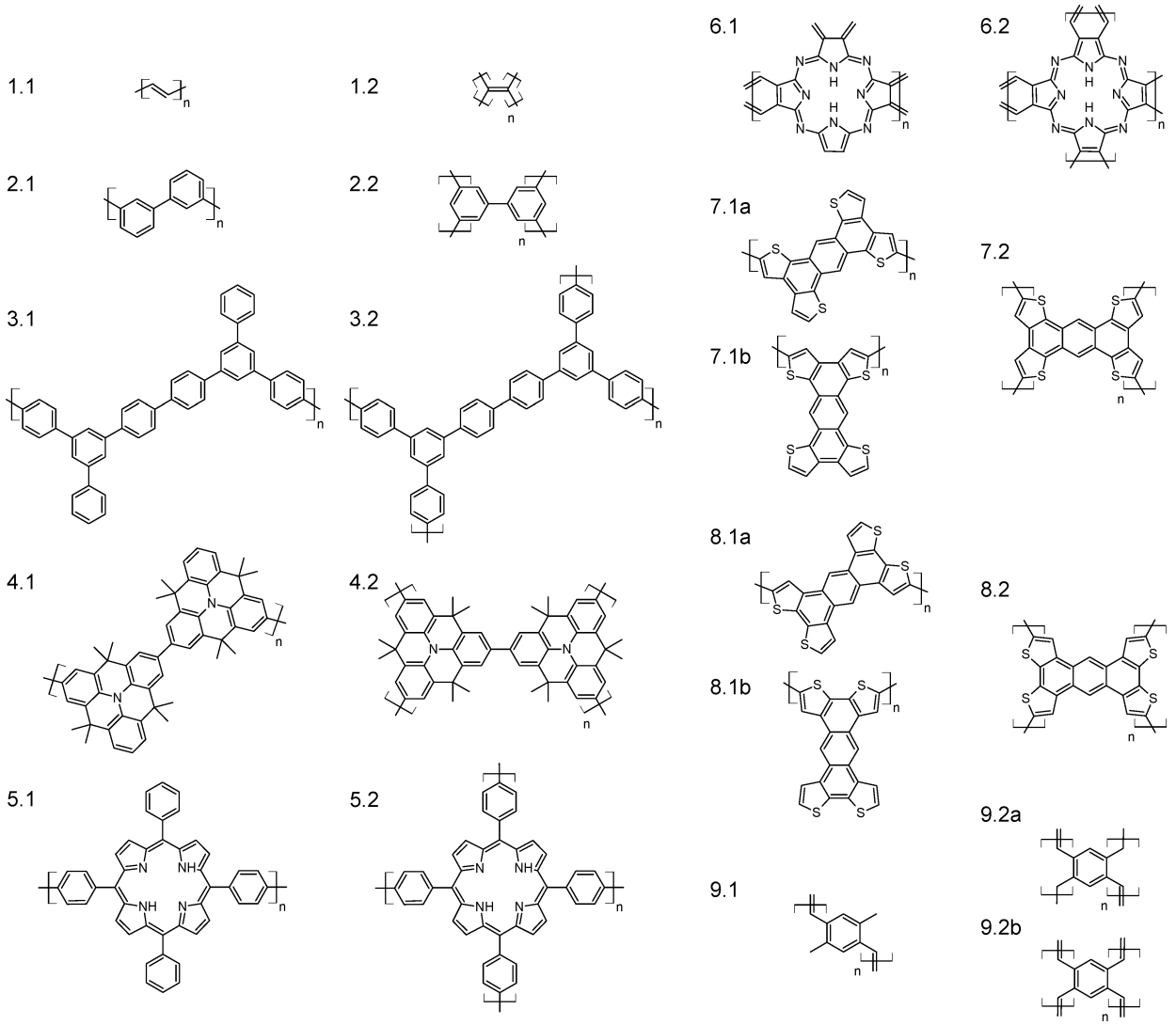

explored 2D conjugated polymers. For the first time, we show how the HLG evolves in 2D conjugated structures as a function of oligomer size. This is particularly important because the current experimental approaches can only afford 2D polymer clusters of a limited size. Comparing the behavior of the currently known 2D polymers to their analogous 1D counterparts (**1**−**7**, Scheme 1), we reveal the interplay between the dimensionality and the "effective conjugation" on the band gap of conjugated polymers.

METHODS

Density functional theory with the B3LYP functional and the 6-31G(d) basis set was used to optimize the geometry of several 1D and 2D oligomers/polymers (Gaussian09 software package[52]). Commonly, the highest possible symmetry was applied to each structure, and atoms were free to relax in a plane. For the two systems **3** and **5** (cf. Scheme 1), torsional degrees of freedom allow for energetically optimal geometries that are nonplanar.[53] For these polymers, different torsional angles were calculated to gain information on the dependence of the HOMO−LUMO gap on nonplanarity. Nonplanar lower-energy conformations also exist for the oligomers of **2** (as well as poly(*m*-phenylene) represented by structure **2.1**); only planar conformations, however, were analyzed to allow comparisons with the fully planar 2D polymer **2.2**. The energy difference of the HOMO and the LUMO is calculated to yield the HLG. The combination of B3LYP functional and 6-31G(d) basis set is reported to perform reasonably well to predict the HLG of organic polymers[16] and seems to circumnavigate the commonly encountered underestimation of the band gap for 3D metals and semiconductors.[54] Our calculated values might differ from experimental values, and care must be taken in interpreting absolute numbers. The quantitative trends we report however, in particular, the different saturation of the HLG in 2D versus 1D, are expected to be observable in experiment.

For one system (**1**), the calculations were also performed with the Hartree−Fock method (HF), DFT with the PBE functional, and with time-dependent DFT, always using the 6-31G(d) basis set. HF is known to overestimate HLGs, and pure DFT with the PBE functional underestimates the HLG.[54] The hybrid functional B3LYP predicts more reasonable gaps, as confirmed by time-dependent DFT (see also Figure 1c,d).

We note that periodic boundary condition calculations of graphene (**1.2**) did not converge, which appears as a general limitation of hybrid functionals for systems with a vanishing band gap. In this case, the comparisons were based on calculations of large oligomers (up to 200 carbons).

The molecular repeat units of 1D and 2D polymers were constructed based on crystallographic considerations: the unit cell of the 1D polymer equals the unit cell of the 2D polymer, in which one lattice vector is removed and C−C bonds connecting previously adjacent cells are replaced by C−H bonds. Consequently, 1D and 2D

dx.doi.org/10.1021/ja408355p | J. Am. Chem. Soc. 2013, 135, 16585−16594

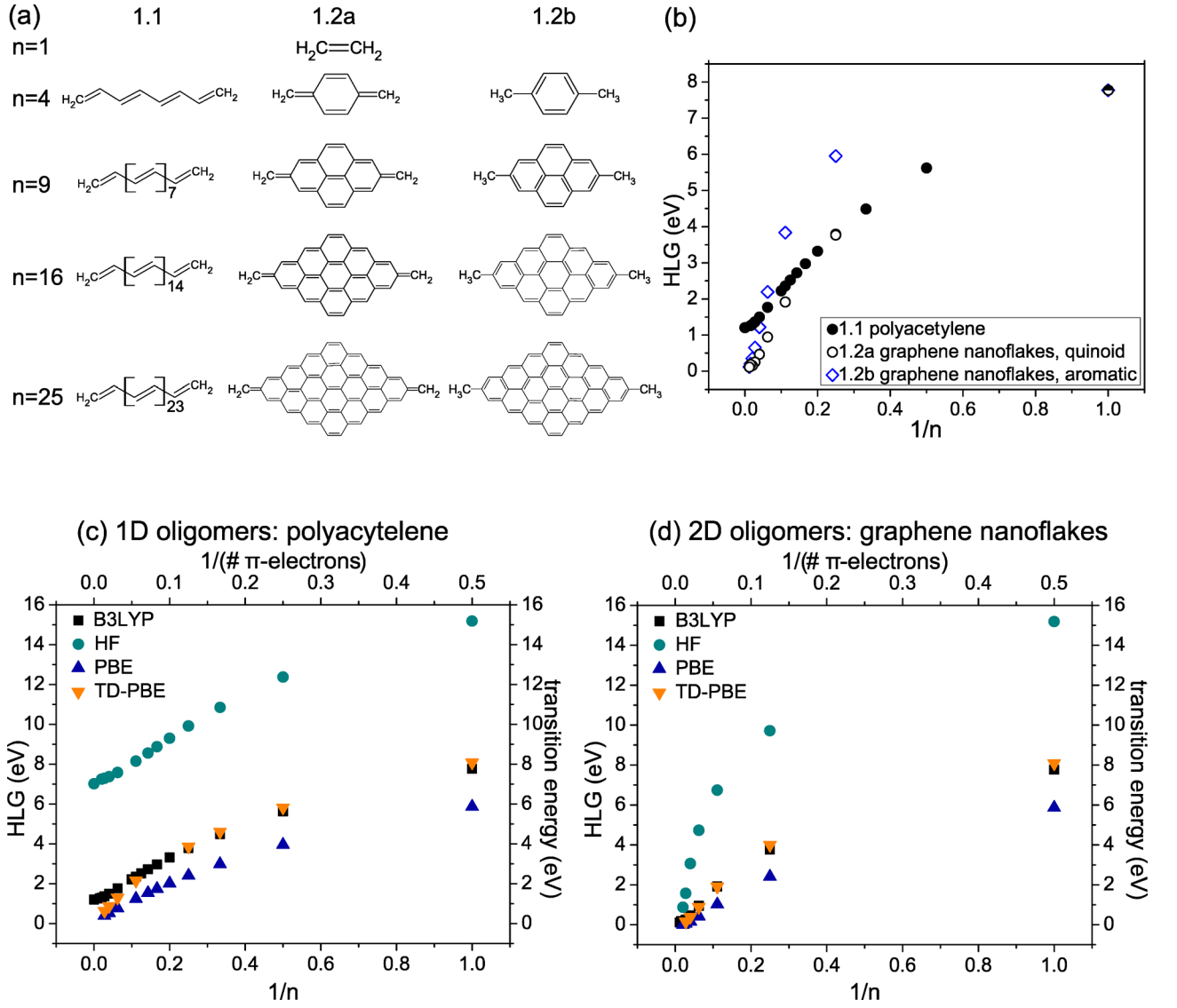

Figure 1. (a) Construction of 1D and 2D polymers from vinylene repeat unit (n = 1) exemplified for n = 4, 9, 16, and 25. (b) HLG for polyacetylene (**1.1**, filled circles), quinoid graphene nanoflakes (**1.2a**, open circles), and aromatic graphene nanoflakes (**1.2b**, blue diamonds) at the B3LYP/6-31G(d) level of theory. Comparison of the HLG (transition energy) at four different levels of theory (HF, DFT/B3LYP, DFT/PBE, left axis; and time-dependent DFT/PBE, right axis) for polyacetylene in (c) and graphene nanoflakes in (d).

unit cells have the same number of atoms in the unit cells, except for additional H atoms. This conserves the number of π-electrons in the unit cells and facilitates the direct comparison of oligomers of a given number of repeat units n. Oligomers are constructed as n repeating unit cells along the lattice vector in 1D or as $\sqrt{n} \times \sqrt{n}$ unit cells ($\sqrt{n}$ repeat units along each of the two lattice vectors) in 2D. This construction principle in 2D leads to extended continuous sheets of repeat units with four nearest neighbors each (except for the terminal repeat units that define the edge of the polymer; see Figure 1a and models in Figure 2a).

RESULTS AND DISCUSSION

HLGs have been calculated for structures whose synthesis was previously reported in literature (Scheme 1): graphene (**1**),[55−57] porous graphene (**2**)[32] and its extended analogue (**3**),[43,58] fused poly(triphenylamine) (**4**),[41,59] poly(tetraphenylporphyrin) (**5**),[39,60,61] poly(phthalocyanine) (**6**),[42] and isomeric poly(tetrathienoanthracene)s (**7**, **8**).[51] Poly(phenylene vinylene) (**9**) has not yet been realized in 2D, although it is one of the most studied 1D conjugated polymers,[62] and a 3D (disordered) microporous polymer, represented by the structure **9.2b**, was reported.[63] The molecular repeat units of these oligomers and polymers have an extended system of π-electrons which facilitates extended conjugation of both 1D and 2D oligomers. Extension of the electronic conjugation is manifested as a reduction of the HLG with increasing oligomer size with its smallest value expected for the infinite polymer.

The HLGs of **1.2a** representing graphene nanoflakes and **1.1** representing one-dimensional polyacetylene oligomers were calculated to test our methodology (Figure 1a). Graphene itself is a material with zero band gap, while graphene flakes exhibit nonzero HLGs which depend on the size of the flakes and the topology of their edges.[64] With increasing number n of repeat units in the polyacetylene oligomer, the HLG diminishes as expected[15,17] (Figure 1b). The slope at which the HLG is reduced is not constant but decreases with increasing oligomer length. This is a behavior described for other 1D conjugated oligomers,[15,65] and we observe it likewise for all other 1D structures (vide infra). The predicted HLGs for the infinite

dx.doi.org/10.1021/ja408355p | J. Am. Chem. Soc. 2013, 135, 16585−16594

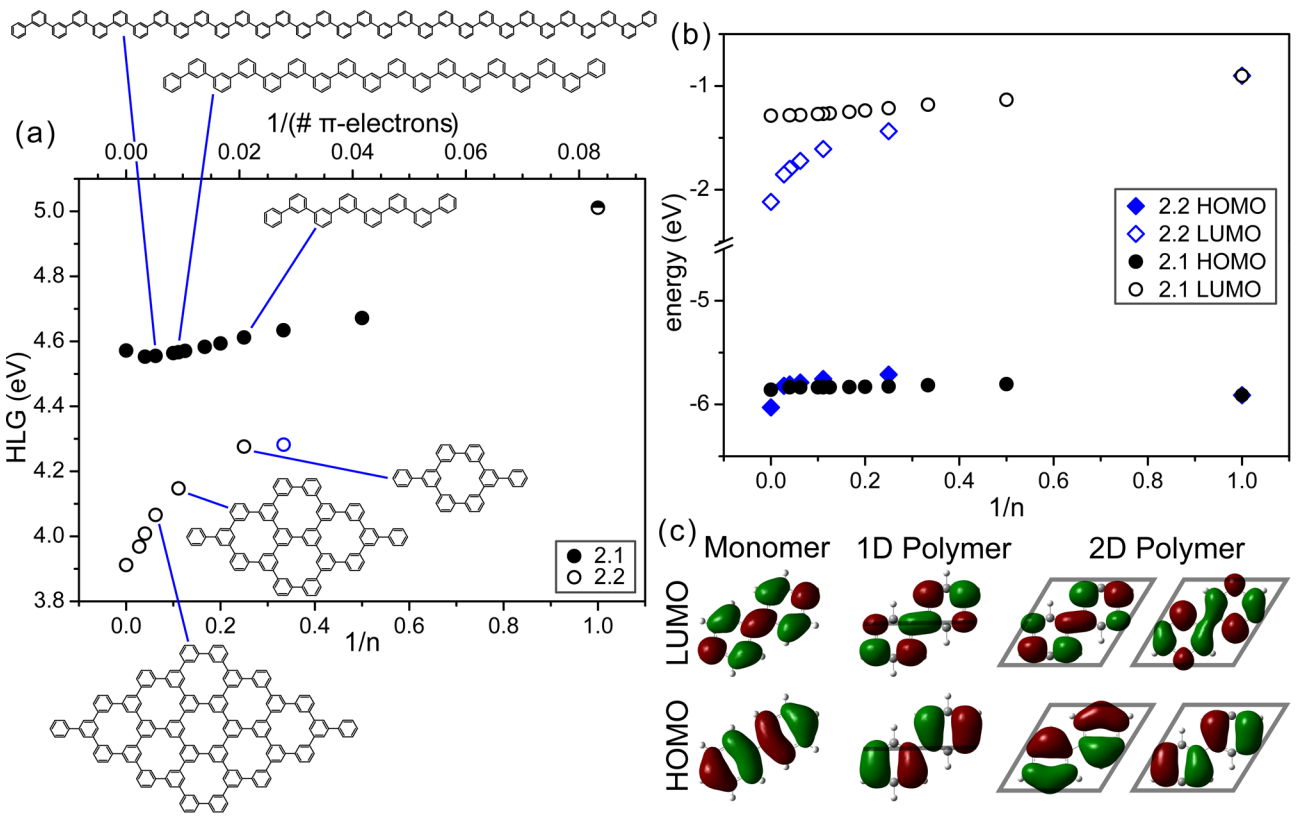

Figure 2. (a) HLG for oligomers **2.1** and **2.2** with exemplary oligomers for n = 4, 9, and 16. HLG of cyclohexa-*m*-phenylene as blue circle. (b) HOMO and LUMO energies of **2.1** and **2.2** oligomers. (c) Molecular orbitals for **2.1** and **2.2** and their molecular repeat unit. Both HOMO and LUMO in 2D are two-fold degenerate.

polyacetylene **1.1** chain (1.20 eV) are in reasonable agreement with the experimental value (optical gap, ~1.4 eV[10]). Connecting the vinylene (CH═CH) repeat units in 2D to form graphene sheets (**1.2a**) also reduces the HLG, but with a slope larger than in 1D. For n = 4, the HLG is about the same in 1D (octatetraene) as in 2D (quinodimethane). For larger n, the gap is consistently smaller in 2D. It is noteworthy that the reduction in the HLG is faster in 2D than in 1D. In fact, the slope of HLG reduction increases in 2D, while in 1D it decreases. Note that having vinylene as a repeat unit leads to a quinoid structure in the 2D oligomers, which significantly perturbs the electronic structure with respect to the aromatic system. For comparison, aromatic graphene nanoflakes have also been calculated (**1.2b**, with CH_3 termini; see Figure 1b), which shows the same qualitative behavior, although with larger HLGs than in the quinoid structure. Both quinoidal and aromatic nanoflakes converge at $n\rightarrow\infty$.

The hybrid B3LYP functional together with the 6-31G(d) basis set have been shown to give HLGs that compare well to experimental values.[16] This is attributed to a cancellation of errors: Hartree−Fock theory overestimates band gaps because charge is calculated to be too localized in the structure, while pure DFT favors a stronger delocalization of the charge and thus underestimates band gaps. B3LYP as a hybrid with contributions from both theories compensates one with the other and predicts band gaps with reasonable accuracy.[16,54] To independently validate that the different behavior of HLG contraction in 2D is not a (hybrid) DFT artifact of the B3LYP functional, we also tested the pure DFT PBE functional (specifically developed for periodic systems) and also performed calculations at the Hartree−Fock (HF) level (Figure 1c,d). We additionally compared the HLG to first excitation energies calculated by time-dependent DFT calculations (with the PBE functional). As expected, the absolute numbers are different, and the HLG is estimated to be larger in HF than in DFT. The general trend, however, of a more rapid decrease in HLG in 2D than in 1D for large oligomers is reproduced at all levels. The numbers from B3LYP agree nicely with those acquired from time-dependent calculations, giving further support for our approach.

Porous graphene **2.2** is a simple, fully planar, and experimentally realized 2D conjugated polymer.[32] Its synthesis was achieved by Ullmann-type coupling of halogenated cyclohexa-*m*-phenylene under ultrahigh vacuum conditions on crystalline surfaces such as Ag(111), Au(111), and Cu(111). It is a cross-conjugated polymer since connecting phenyl rings at their *meta* positions does not allow for direct conjugation (a pathway of alternating single and double bonds).[18] This explains the large ~4.6 eV HLG gap even in the planarized[66] poly(*m*-phenylene) (**2.1**) which only contracts by 0.4 eV from the single molecular repeat unit to infinite 1D polymer (Figure 2a, black filled circles). An optical HLG of ~4.0 eV was reported for **2.1** in the solid state.[67] The HLG contraction is realized in **2.1** almost exclusively due to stabilization of the LUMO; the HOMO is only raised for n = 2, followed by a very small but steady decrease (stabilization) at higher n (Figure 2b). The latter is likely an end-group effect: replacing electropositive hydrogens at the oligomer termini with electronegative sp^2-carbons affects HOMO more than does extension of the (cross-)conjugated chain (see Supporting Information for fluorine-terminated oligomers of **2**). This may also explain the slight *increase* of HLG for the infinite polymer

dx.doi.org/10.1021/ja408355p | J. Am. Chem. Soc. 2013, 135, 16585−16594

(the lowest HLG is predicted for phenylene 50-mer, n = 25, HLG = 4.55 eV).

On the other hand, the oligomers **2.2**, despite having the same *meta* connectivity of **2.1**, show a more considerable reduction of the HLG of 1.1 eV (open circles). The HOMO of **2.2** experiences an even larger stabilization (Figure 2b), but the overall HLG contraction is achieved due to the more dramatically stabilized LUMO.

Apparently, the direct versus cross-conjugation paradigm of the valence bond theory, commonly invoked in discussing linearly conjugated systems, is not necessarily applicable in 2D. An explanation for why the HLG of **2.2** is reduced compared to **2.1** can be found by looking at their respective molecular orbitals (Figure 2c). In **2.1**, nodes centered on carbon atoms in HOMO and LUMO spatially separate the wave function as an effect of cross-conjugation. In **2.2**, the HOMO and LUMO are two-fold degenerate and have contributions to the wave function without nodes on carbon atoms, thus enhancing conjugation. Clearly, the mixing of monomer MO in 2D is different from that in 1D, as also seen in the topology of the frontier orbitals in corresponding oligomers (Supporting Information). The lower HLG in 2D can be tracked back to the cyclohexa-*m*-phenylene moieties. The first ring closes for n = 4 and already has a significantly smaller HLG than any **2.1** oligomer or polymer. For comparison, the purely six-membered cyclohexa-*m*-phenylene ring has a HLG of 4.28 eV, the same as **2.2** with n = 4 (Figure 2a, blue circle). Additional rings for larger n in **2.2** further reduce the HLG.

An extended version of porous graphene with larger pore size (**3.2**) has been synthesized in a surface-confined reaction from 1,3,5-tris(*p*-bromophenyl)benzene under similar conditions as structure **2.2**.[43,58] Structure **3** shows almost no variation in HLG from monomer to 1D or 2D polymer (Figure 3). Fully

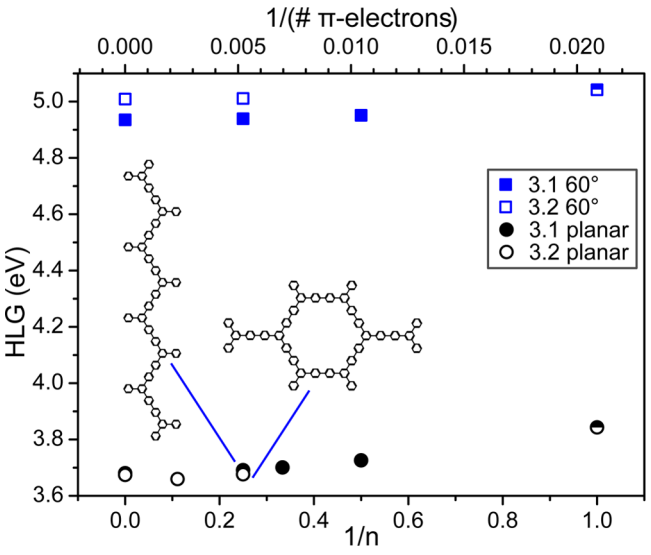

Figure 3. HLG of oligomers **3.1** and **3.2** in the planar and the fully relaxed twisted conformation.

relaxed geometries of **3** yield a dihedral angle between phenyl rings of ∼60° (blue squares). The somewhat lower HLG of **3.1** versus **3.2** in the fully relaxed conformation stems from the peripheral phenyl groups, which form a smaller torsional angle of 30° with the central phenyl rings, thus enhancing π-overlap. For better comparison between the planar polymer **2** and polymer **3**, all phenyl rings in **3** were forced into a coplanar geometry. This structure is less stable than the fully relaxed conformation, by 0.47 eV per repeat unit (0.06 eV per phenyl−phenyl torsion) in the 1D and by 0.35 eV (0.04 eV per phenyl−phenyl torsion) in the 2D polymer in vacuum, but could be feasible in surface-adsorbed layers. The rotational barrier of biphenyl is calculated to be 0.09 eV at the same level of theory and is small enough to allow planar adsorption on Cu(111).[68] We infer that **3.2** likely adopts a coplanar geometry as well when adsorbed on surfaces as described in experiments.[43,58] As a result of the increased overlap of the π-orbitals,[69] the predicted HLG of **3** is lowered by over 1.2 eV comparing to the 60° twisted geometry (black circles, Figure 3). The HLG in planar **3** is dominated by the four phenyl rings connected at their *para* positions which allows for direct conjugation and thus defines the maximal effective conjugation length[67] (the HLG of *p*-quaterphenyl at the same level of theory is 3.90 eV for the planar molecule and 5.28 eV for the 60° twisted molecule). Additional spreading of conjugation through cross-conjugated *meta*-connected sites has only a minor impact on the HLG.

Nitrogen-containing structures **4** have been synthesized as a 2D polymer **4.2** in the surface-confined coupling of a brominated triphenylamine derivative[41] and in solution as macrocyclic and linear oligomers.[59] Triarylamine oligomers are widely used as hole-transporting materials in organic light-emitting diodes.[70] However, the conjugation via the lone pair of the nitrogen (−N:−) is generally considered to be less effective (no pathway of alternating single and double bonds). Accordingly, the HLG gap reduction in **4** is relatively small (∼0.4 eV in 1D and ∼0.6 eV in 2D, Figure 4a). As in the

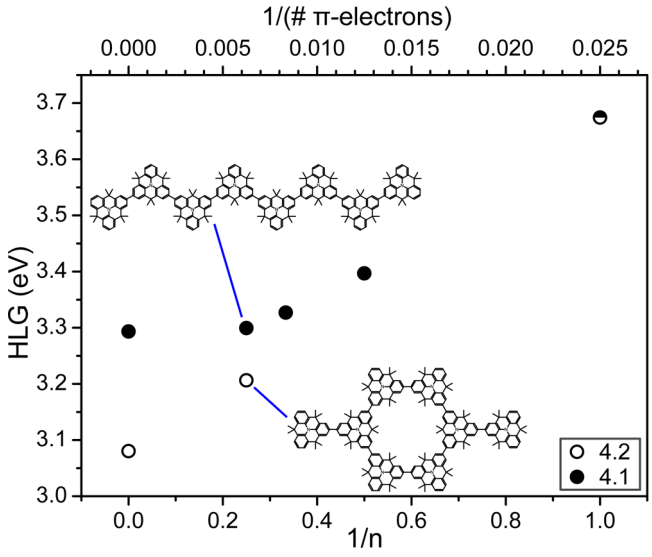

Figure 4. HLG for structure **4**.

porous graphene **2**, the predicted HLGs of the infinite 2D sheet (**4.2**, 3.08 eV) are smaller than that of the (infinite) 1D chain (**4.1**, 3.29 eV). Compared to the optical gaps, E_g, of the corresponding oligomers,[59] the theory overestimates the HLG by ∼0.3 eV.

Poly(tetraphenylporphyrin) **5.2** was the first formally conjugated 2D polymer synthesized by surface-templated dehalogenating coupling.[39] The efficient conjugation *within* the porphyrin moiety defines the relatively low HLG already achieved for the monomer. Increasing the number of monomer

dx.doi.org/10.1021/ja408355p | J. Am. Chem. Soc. 2013, 135, 16585−16594

units causes very little change of the HLG (Figure 5a). This is primarily due to a large torsional angle of the phenyl rings

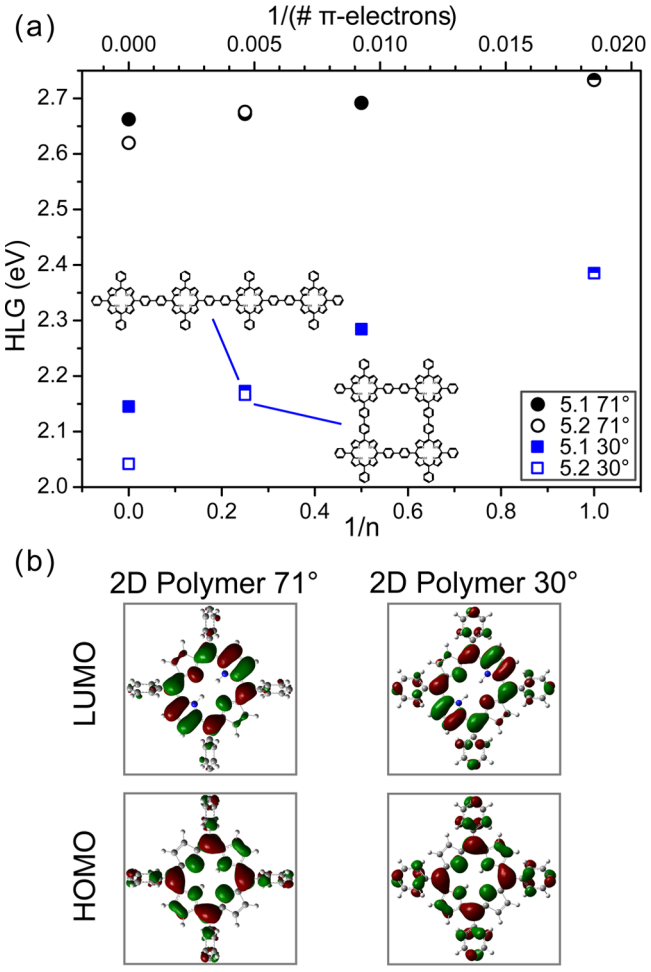

Figure 5. (a) HLG for oligomers **5.1** and **5.2** in the fully relaxed (71° between phenyl rings and porphyrin core) and partially planarized (30°) conformation. (b) Molecular orbitals for 5.2.

(71°) with respect to the porphyrin core (Figure 5a, black circles). It is expected that the twisting in the surface-adsorbed polymer will be reduced compared to the gas-phase-calculated geometry to maximize the interaction with the surface, although full planarization is not possible due to severe steric repulsions between the phenyl and pyrrole moieties. The energy penalty to reduce the twisting of the four phenyl ring from 71 to 30° is 2.73/2.46 eV (in the monomer/2D polymer; in all calculations, the porphyrin core was fixed to be planar). This corresponds to 0.68/0.62 eV per phenyl ring and is significantly larger than the rotational barrier found in **3.2** (0.04 eV). Unlike **3.2**, **5.2** is not expected to be able to adopt a planar conformation.

For oligomers with a 30° twist angle (Figure 5a, blue squares), the enhanced π-overlap reduces the HLG by ~0.35–0.65 eV and leads to faster HLG contraction with increasing n. For both 30 and 71° structures, the lowest HLG is achieved for the infinite polymer **5.2**, which again shows the more efficient conjugation in the 2D versus 1D system. However, the overall electron delocalization in **5** is limited by the misalignment of the π-orbitals at the twisted inter-ring connections. Figure 5b shows the molecular orbitals for the 2D polymer in its 71 and 30° geometry. The decreased torsional angle leads to increased frontier orbital density on the phenyl groups, which leads to a more effective conjugation and thus lowers the HLG of the longer oligomers.

Polyphthalocyanine **6.2** with several direct conjugation pathways was recently synthesized as an iron complex by polycondensation of tetracyanobenzene catalyzed by atomic Fe on Au(111), Ag(111), and on NaCl/Ag(110) surfaces.[42] It is the only ladder-type 2D conjugated polymer reported to date. The exceptional electronic coupling through fused phenylene rings results in a very good electronic conjugation, thus leading to very small HLGs. In the metal-free polyphthalocyanine, the gap is contracted by ~1 eV in the 1D polymer **6.1** and by ~1.7 eV in the 2D polymer **6.2a** versus the molecular repeat unit (Figure 6a). The principal difference in the HLG evolution in

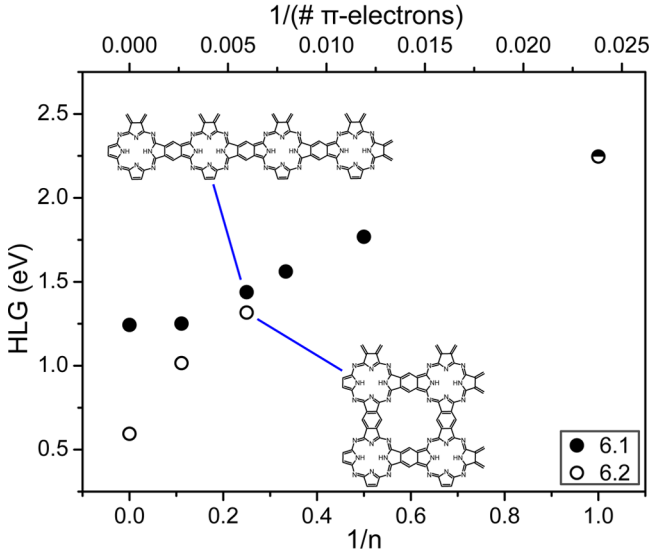

Figure 6. (a) HLG for metal-free oligomers/polymers **6.1** and **6.2**.

1D and 2D conjugated systems is very clear: at increasing n, the HLG "saturates" in 1D polymers, but in 2D polymers, it displays an accelerated contraction. Polyphthalocyanine is predicted to possess the lowest HLG (~0.6 eV for the metal-free polymer, probably even lower in its iron complex, **6.2-Fe**) among all experimentally realized 2D π-conjugated polymers (except for graphene). The iron polyphthalocyanine repeat unit (**6-Fe**, n = 1) has a lower HLG (1.48 eV) compared to **6** (2.25 eV), which is primarily due to significant stabilization of the LUMO (see Supporting Information). Its polymers are also expected to have lower HLGs. Plane-wave calculations with the PBE functional were reported to yield a band gap of 0.29 eV for **6.2** and a band gap of 0.24 eV for **6.2-Fe**, which was also shown to be antiferromagnetic.[71]

Thiophene-based polymers **7** have been synthesized from brominated tetrathienoanthracene (TTA) in an Ullmann coupling on Ag(111).[51] Lower aromatic stabilization energy of the thiophene repeat unit (compared to benzene) generally leads to more efficient conjugation in 1D conjugated polythiophenes. The absolute majority of semiconducting polymers, particularly those with low HLG, are thiophene-based.[2] The TTA repeat unit was designed to have conjugation pathways as alternating single and double bonds in two directions (which can be denoted as *para* or *ortho* versus the central benzene ring). However, in contrast to all previously discussed cases, the two pathways are not electronically

dx.doi.org/10.1021/ja408355p | J. Am. Chem. Soc. 2013, 135, 16585–16594

equivalent. Indeed, 1D polymerization along the *para* direction (**7.1a**) appears to result in a much more pronounced HLG contraction comparing to *ortho* 1D polymer **7.1b** (Figure 7).

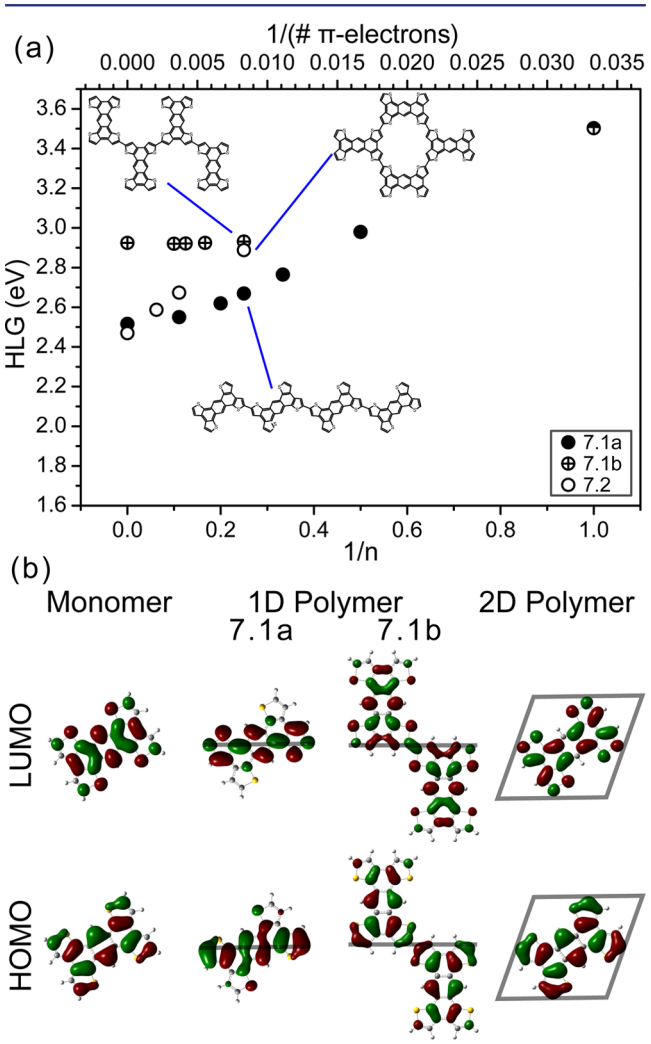

Figure 7. (a) HLG gap for the tetrathienoanthracene **7**. (b) HOMO and LUMO for monomer, 1D polymers **7.1a** and **b**, and 2D polymer.

The 2D polymer **7.2** contains both conjugated pathways, and its HLG is dictated by their combination. For all calculated oligomers ($n \leq 16$), the HLG of **7.2** is between that of **7.1a** and **7.1b**, although the faster HLG contraction in 2D affords the polymer **7.2** ($n = \infty$) a lower HLG (2.47 eV) than those of both 1D polymers.

Interestingly, a slight change in the structure of the TTA building block (position of sulfur atoms) does not significantly perturb the MOs of the monomers but creates a remarkable change in the conjugation efficiency. Polymer **8.2** has a lower HLG than **7.2** and a different trend of HLG contraction is found in the corresponding 1D polymers. The conjugation through *para* positions is slightly more effective in **7.1a** than in **8.1a**, while the connection through *ortho* positions is much more efficient in **8.1b** compared to that in **7.1b**. This correlates well with the conjugation pathways through the thiophene ring: the electronic coupling is more efficient in the chains running through 2,5-connected thiophene (**7.1a**, **8.1b**) than through 2,4-connected thiophene (**7.1b**, **8.1a**). The observed behavior can also be rationalized from the molecular orbitals in Figures 7b and 8b. Nodes in the wave function on the central benzene ring appear in **7.2** that are absent in either the monomer or

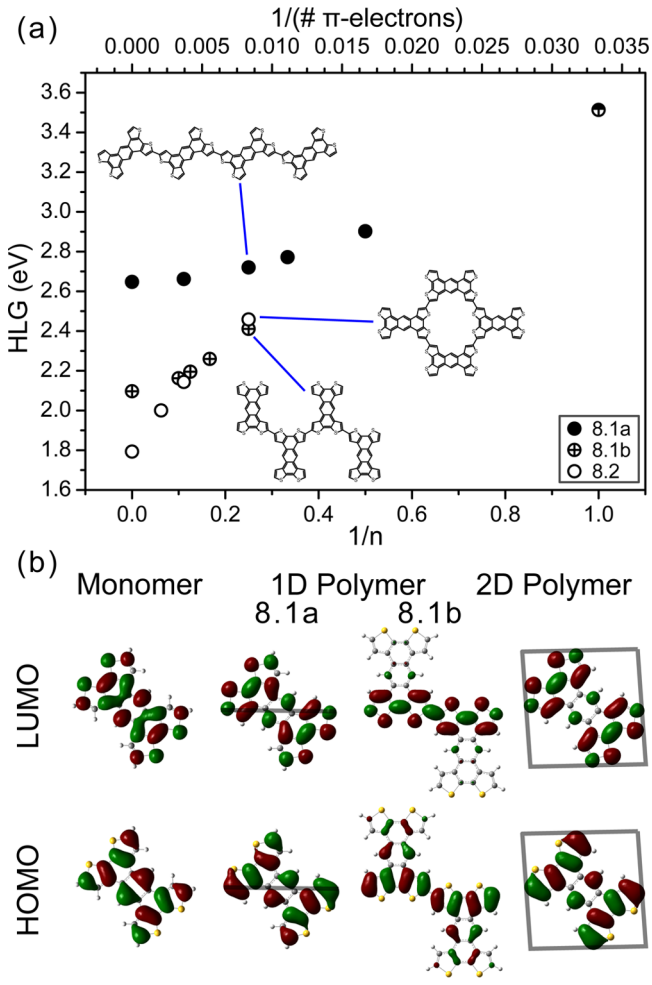

Figure 8. (a) HLG gap for the tetrathienoanthracene **8**. (b) HOMO and LUMO for monomer, 1D polymer **8.1a** and **b**, and 2D polymer.

7.1a, thus interrupting the efficient conjugation pathway through *para* positions. These nodes are already observable in **8.1a**, increasing the HLG with respect to **7.1a**. Although nodes are also present in **8.2**, efficient conjugation through both of the two *ortho* connections (as apparent from **8.1b**) lowers the HLG significantly. As a result of the multiple conjugation pathways in two dimensions, the 2D poly(TTA) **8.2** shows a much smaller HLG compared to the 1D analogues **8.1a** and **8.1b** (Figure 8) and also smaller than that of the isomeric poly(TTA) **7.2**. Small changes in the chemical structure thus significantly modify the electronic structure and hence lead to different HLGs.

A remaining question is how the HLG behaves in a 2D polymer that is not fully conjugated. We have investigated this point by calculating various poly(phenylene vinylene) derivatives. **9.1** has a 1D conjugated pathway as found in common PPV oligomers/polymers.[62] **9.2a** is a two-dimensional structure with 1D conjugation (PPV chains are electronically separated by saturated ethylene bridges), with a 2,5-dimethylstyrene repeat unit as in **9.1**. **9.2b** is a fully 2D conjugated polymer with 1,2-divinylbenzene repeat unit; its disordered equivalent has been synthesized as a microporous polymer.[63] Our approach to constructing oligomers here is slightly different to allow

dx.doi.org/10.1021/ja408355p | J. Am. Chem. Soc. 2013, 135, 16585−16594

comparison between the three structures (different repeat units have to be used, and thus the number of π-electrons per repeat unit is not the same). Connecting benzene rings in *ortho* and *para* positions as in **9.2b** allows for direct conjugation with reduction in the HLG, as opposed to polymers **2** and **3** which are only cross-conjugated. The 1D oligomers of **9.1** exhibit subsequent significant lowering of the HLG with increasing n, down to 2.25 eV for the infinite polymer (cf. experimental $E_g \sim$ 2.45 eV for poly(2,6-dialkylphenylene-1,4 vinylene)s[62]). The HLG of **9.2a** converges to almost the same HLG as **9.1** (Figure 9a). The longest conjugation pathway of **9.2a** is given by the

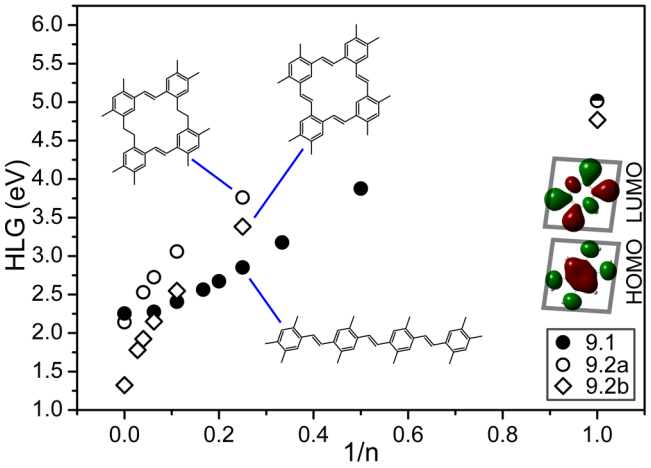

Figure 9. HLG for the phenylene-based oligomers/polymers **9** and the repeat units 2,5-dimethylstyrene (half-shaded circle) and 1,2-divinylbenzene (diamond at $1/n = 1$). HOMO and LUMO of **9.2b** as inset.

side length of the 2D polymer and scales with $\sqrt{n}$. This causes the different shape of the HLG versus $1/n$ plots for **9.1** and **9.2a**, which, however, nearly coincide when the number of conjugated units is used as the function's argument (see Supporting Information). The fully conjugated 2D polymer **9.2b** has a HLG (1.32 eV) considerably lower than that of **9.1**, as expected from its fully 2D delocalized orbitals (Figure 9, inset). However, a slightly (by ~0.1 eV) lower HLG of **9.2a** oligomers/polymer compared to **9.1** is unexpected. It can be traced back to a small degree of spreading conjugation through sp^3 bonds (hyperconjugation) causing a "cross-talk" of the neighboring poly(*p*-phenylene vinylene) strands (see Supporting Information).

A summary of the energies of the HOMO, the LUMO, and the HLG for the 2D polymers, along with their unit cell parameters, is given in Table 1. The HLG depends greatly on the molecular repeat unit. The contraction of the HLG from repeat unit over 1D polymer to 2D polymer is shown in Table 2. In all cases is the HLG of the 2D polymer smaller than the gap of the 1D polymer.

The studied 2D polymers can be classified according to their symmetry. Networks **1.2**, **2.2**, **3.2**, and **4.2** contain tridentate, trifold symmetry nodes which form a hexagonal lattice. Typically, such polymers are cross-conjugated, although not without exceptions (notably, graphene **1.2**). This is manifested in a relatively large band gap in the studied examples. Tetradentate, tetrafold symmetry nodes, as in polymers **5.2** and **6.2**, form a square lattice which can display direct conjugation in all directions (omniconjugation). Except when limited by the internal structure of the monomer (as in **5.2**), such networks display a large HLG reduction; the lowest HLG

Table 1. Lattice Parameters of the Optimized 2D Polymers along with the Energies of Their HOMO, LUMO, and HLG

structure	ref	a (nm)	b (nm)	γ (deg)	HOMO (eV)	LUMO (eV)	HLG (eV)
2.2	32	0.75	0.75	60	−6.03	−2.12	3.91
3.2[a]	43, 58	2.27	2.27	60	−5.51	−1.84	3.67
4.2	41, 59	1.75	1.75	60	−4.24	−1.16	3.08
5.2[b]	39, 60	1.71	1.71	90	−4.96	−2.34	2.62
6.2	42	1.07	1.07	90	−4.50	−3.91	0.59
7.2	51	1.21	1.21	71	−5.17	−2.70	2.47
8.2		1.16	1.16	97	−4.72	−2.93	1.79
9.2a		0.668	0.671	82	−4.82	−2.68	2.14
9.2b	63	0.67	0.67	99	−4.64	−3.31	1.32

[a]Planar geometry. [b]Optimal 71° angle between phenyl rings and porphyrin.

(0.59 eV) was calculated for **6.2**. However, the molecular design of monomers for such systems is currently limited to porphyrin and phthalocyanine. In contrast, tetradentate, bifold symmetry nodes can be realized with a number of different molecular building blocks, as exemplified in the polymers **7.2**, **8.2**, and **9.2b**. They typically arrange into oblique lattices, also with direct conjugation pathways and considerable HLG reduction upon 2D polymerization. However, the same molecular building block can be linked to form 2D polymers with different topology and symmetry. For example, repeat unit **7**, for which we already discussed two 1D polymers (**7.1a** and **7.1b**) of different topology, can form conjugated 2D polymers with oblique, hexagonal, or square lattice (Figure 10). On one hand, such variance is likely to lead to structural disorder, as observed in the synthesis of **7.2**.[51] On the other hand, it also creates an opportunity for further engineering of the electronic structure and creating anisotropic 2D materials.

CONCLUSIONS

We have presented hybrid DFT calculations of the electronic structure for a series of the experimentally realized two-dimensional conjugated polymers. Our results show that the HLG of 2D conjugated polymers is always smaller than that of their 1D counterpart (Table 2). However, the difference between them depends critically on the connectivity between the repeat units and in the studied examples varied from <0.1 eV (for **3**) to ~1 eV (for **6** and **9**).

Comparing the evolution of the HLG with the increasing length of oligomers, we provide evidence that the contraction of the HLG follows a different convergence behavior: while in 1D the HLG reduction becomes smaller for each additional repeat unit, in 2D the HLG contraction becomes faster for increasing oligomer size. This can be related to the number of the connections (conjugated links k) that scales linearly with the oligomer length in 1D ($k = n - 1$) but superlinearly in 2D ($k = 2\sqrt{n}(\sqrt{n} - 1)$).

As is the case in 1D systems, coplanarity of conjugated units strongly affects the electron delocalization in 2D polymers. The 2D polymers in which π-overlap is hindered by torsional twisting (**3** and **5**) reveal larger HLG and smaller HLG contraction with increasing oligomer size than their planarized analogues. The effect of cross-conjugation (which explains better electron delocalization via, e.g., 1,4-phenylene and 2,5-thienylene as compared to 1,3-phenylene and 2,4-thienylene)

dx.doi.org/10.1021/ja408355p | J. Am. Chem. Soc. 2013, 135, 16585−16594

Table 2. Energies of the Occupied and Unoccupied Orbitals of the Monomer, 1D Polymer, and 2D Polymer

	HOMO repeat unit	LUMO repeat unit	HLG repeat unit	HOMO 1D	LUMO 1D	HLG 1D	HOMO 2D	LUMO 2D	HLG 2D
2	−5.91	−0.90	5.01	−5.86	−1.29	4.57	−6.03	−2.12	3.91
3[a]	−5.46	−1.62	3.84	−5.42	−1.74	3.68	−5.51	−1.84	3.67
4	−4.49	−0.82	3.67	−4.32	−1.02	3.29	−4.24	−1.16	3.08
5[b]	−4.92	−2.19	2.73	−4.92	−2.26	2.66	−4.96	−2.34	2.62
6	−5.03	−2.78	2.25	−4.72	−3.48	1.24	−4.50	−3.91	0.59
7	−5.29	−1.79	3.50	−4.93[c]	−2.41[c]	2.52[c]	−5.17	−2.70	2.47
8	−5.20	−1.69	3.51	−4.89[c]	−2.24[c]	2.65[c]	−4.72	−2.93	1.79
9a	−5.82	−0.82	5.01	−4.54	−2.28	2.25	−4.82	−2.68	2.14
9b	−5.85	−1.08	4.76				−4.64	−3.31	1.32

[a]Planar geometry. [b]Optimal 71° angle between phenyl rings and porphyrin. [c]One-dimensional polymer type a (**7.1a** and **8.1a**).

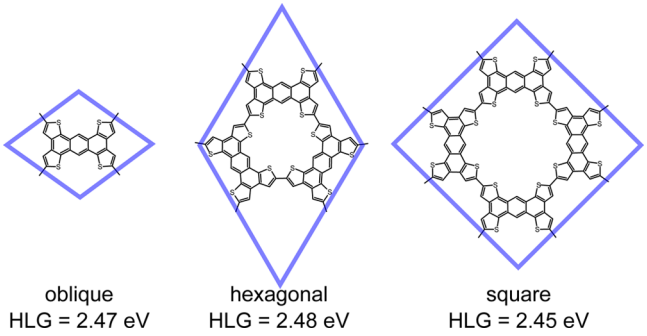

Figure 10. Three 2D polymers of different topology (with oblique, hexagonal, and square lattice) constructed from building block **7**.

on HLG contraction in 2D can be less detrimental than in 1D, as demonstrated by significant HLG contraction in the fully cross-conjugated porous graphene **2.2**.

The experimental work on the synthesis of 2D conjugated materials as surface-supported monolayers, covalent organic frameworks, conjugated dendrimers, and (disordered) microporous conjugated polymers is rapidly building up. It is now time to explore the electronic properties of such materials and demonstrate if and how they can compete in optoelectronic applications with inorganic 2D materials, such as graphene or GaAs. Our work sheds light on what can be expected from the currently accessible 2D conjugated polymers and shows how tailored HLG can be realized in 2D by suitable structural design and the choice of molecular repeat unit.

■ ASSOCIATED CONTENT

Supporting Information

HOMO and LUMO energies, additional molecular orbitals, *xyz* coordinates of 1D and 2D polymers. Full ref 52. This material is available free of charge via the Internet at http://pubs.acs.org.

■ AUTHOR INFORMATION

Corresponding Authors

r.gutzler@fkf.mpg.de
dmitrii.perepichka@mcgill.ca

Notes

The authors declare no competing financial interest.

■ ACKNOWLEDGMENTS

We wish to dedicate this paper to the memory of Prof. Michael Bendikov (1971−2013). We acknowledge the support by NSERC-Discovery and FQRNT-Team grants, and thank the Centre for Research in Molecular Modeling (CERMM) for access to computational infrastructure.

■ REFERENCES

(1) Shirakawa, H.; Louis, E. J.; MacDiarmid, A. G.; Chiang, C. K.; Heeger, A. J. *J. Chem. Soc., Chem. Commun.* **1977**, 578−580.
(2) *Handbook of Thiophene-Based Materials: Applications in Organic Electronics and Photonics*; Perepichka, I. F., Perepichka, D. F., Eds.; John Wiley & Sons: Chichester, UK, 2009.
(3) Facchetti, A. *Chem. Mater.* **2010**, *23*, 733−758.
(4) Thomas, S. W., III; Joly, G. D.; Swager, T. M. *Chem. Rev.* **2007**, *107*, 1339−1386.
(5) Liu, B.; Bazan, G. C. *J. Am. Chem. Soc.* **2006**, *128*, 1188−1196.
(6) Feng, G.; Ding, D.; Liu, B. *Nanoscale* **2012**, *4*, 6150−6165.
(7) Avouris, P. *Nano Lett.* **2010**, *10*, 4285−4294.
(8) Georgakilas, V.; Otyepka, M.; Bourlinos, A. B.; Chandra, V.; Kim, N.; Kemp, K. C.; Hobza, P.; Zboril, R.; Kim, K. S. *Chem. Rev.* **2012**, *112*, 6156−6214.
(9) Ruffieux, P.; Cai, J.; Plumb, N. C.; Patthey, L.; Prezzi, D.; Ferretti, A.; Molinari, E.; Feng, X.; Müllen, K.; Pignedoli, C. A.; Fasel, R. *ACS Nano* **2012**, *6*, 6930−6935.
(10) Patil, A. O.; Heeger, A. J.; Wudl, F. *Chem. Rev.* **1988**, *88*, 183−200.
(11) Roncali, J. *Chem. Rev.* **1997**, *97*, 173−206.
(12) Beaujuge, P. M.; Reynolds, J. R. *Chem. Rev.* **2010**, *110*, 268−320.
(13) Günes, S.; Neugebauer, H.; Sariciftci, N. S. *Chem. Rev.* **2007**, *107*, 1324−1338.
(14) Izumi, T.; Kobashi, S.; Takimiya, K.; Aso, Y.; Otsubo, T. *J. Am. Chem. Soc.* **2003**, *125*, 5286−5287.
(15) Zade, S. S.; Bendikov, M. *Org. Lett.* **2006**, *8*, 5243−5246.
(16) Zade, S. S.; Zamoshchik, N.; Bendikov, M. *Acc. Chem. Res.* **2010**, *44*, 14−24.
(17) Brédas, J. L.; Silbey, R.; Boudreaux, D. S.; Chance, R. R. *J. Am. Chem. Soc.* **1983**, *105*, 6555−6559.
(18) Van der Veen, M. H.; Rispens, M. T.; Jonkman, H. T.; Hummelen, J. C. *Adv. Funct. Mater.* **2004**, *14*, 215−223.
(19) Baughman, R. H.; Eckhardt, H.; Kertesz, M. *J. Chem. Phys.* **1987**, *87*, 6687−6699.
(20) Narita, N.; Nagai, S.; Suzuki, S.; Nakao, K. *Phys. Rev. B* **1998**, *58*, 11009−11014.
(21) Tanaka, K.; Kosai, N.; Maruyama, H.; Kobayashi, H. *Synth. Met.* **1998**, *92*, 253−258.
(22) Hatanaka, M. *Chem. Phys. Lett.* **2010**, *488*, 187−192.
(23) Kang, J.; Li, J.; Wu, F.; Li, S.-S.; Xia, J.-B. *J. Phys. Chem. C* **2011**, *115*, 20466−20470.
(24) Zhou, J.; Lv, K.; Wang, Q.; Chen, X. S.; Sun, Q.; Jena, P. *J. Chem. Phys.* **2011**, *134*, 174701.
(25) Enyashin, A. N.; Ivanovskii, A. L. *Phys. Status Solidi B* **2011**, *248*, 1879−1883.
(26) Long, M.; Tang, L.; Wang, D.; Li, Y.; Shuai, Z. *ACS Nano* **2011**, *5*, 2593−2600.
(27) Malko, D.; Neiss, C.; Viñes, F.; Görling, A. *Phys. Rev. Lett.* **2012**, *108*, 086804.
(28) Liu, Y.; Wang, G.; Huang, Q.; Guo, L.; Chen, X. *Phys. Rev. Lett.* **2012**, *108*, 225505.

(29) Pan, L. D.; Zhang, L. Z.; Song, B. Q.; Du, S. X.; Gao, H.-J. *Appl. Phys. Lett.* **2011**, *98*, 173102.
(30) Brunetto, G.; Autreto, P. A. S.; Machado, L. D.; Santos, B. I.; dos Santos, R. P. B.; Galvão, D. S. *J. Phys. Chem. C* **2012**, *116*, 12810−12813.
(31) Wang, X.-Q.; Li, H.-D.; Wang, J.-T. *Phys. Chem. Chem. Phys.* **2013**, *15*, 2024−2030.
(32) Bieri, M.; Nguyen, M.-T.; Gröning, O.; Cai, J.; Treier, M.; Aït-Mansour, K.; Ruffieux, P.; Pignedoli, C. A.; Passerone, D.; Kastler, M.; Müllen, K.; Fasel, R. *J. Am. Chem. Soc.* **2010**, *132*, 16669−16676.
(33) Perepichka, D. F.; Rosei, F. *Science* **2009**, *323*, 216−217.
(34) Sakamoto, J.; van Heijst, J.; Lukin, O.; Schlüter, A. D. *Angew. Chem., Int. Ed.* **2009**, *48*, 1030−1069.
(35) Mas-Ballesté, R.; Gómez-Navarro, C.; Gómez-Herrero, J.; Zamora, F. *Nanoscale* **2011**, *3*, 20−30.
(36) Lackinger, M.; Heckl, W. M. *J. Phys. D: Appl. Phys.* **2011**, *44*, 464011.
(37) Franc, G.; Gourdon, A. *Phys. Chem. Chem. Phys.* **2011**, *13*, 14283−14292.
(38) Colson, J. W.; Dichtel, W. R. *Nat. Chem.* **2013**, *5*, 453−465.
(39) Grill, L.; Dyer, M.; Lafferentz, L.; Persson, M.; Peters, M. V.; Hecht, S. *Nat. Nanotechnol.* **2007**, *2*, 687−691.
(40) Zwaneveld, N. A. A.; Pawlak, R.; Abel, M.; Catalin, D.; Gigmes, D.; Bertin, D.; Porte, L. *J. Am. Chem. Soc.* **2008**, *130*, 6678−6679.
(41) Bieri, M.; Blankenburg, S.; Kivala, M.; Pignedoli, C. A.; Ruffieux, P.; Müllen, K.; Fasel, R. *Chem. Commun.* **2011**, *47*, 10239−10241.
(42) Abel, M.; Clair, S.; Ourdjini, O.; Mossoyan, M.; Porte, L. *J. Am. Chem. Soc.* **2011**, *133*, 1203−1205.
(43) Gutzler, R.; Walch, H.; Eder, G.; Kloft, S.; Heckl, W. M.; Lackinger, M. *Chem. Commun.* **2009**, 4456−4458.
(44) Dienstmaier, J. F.; Gigler, A. M.; Goetz, A. J.; Knochel, P.; Bein, T.; Lyapin, A.; Reichlmaier, S.; Heckl, W. M.; Lackinger, M. *ACS Nano* **2011**, *5*, 9737−9745.
(45) Tanoue, R.; Higuchi, R.; Enoki, N.; Miyasato, Y.; Uemura, S.; Kimizuka, N.; Stieg, A. Z.; Gimzewski, J. K.; Kunitake, M. *ACS Nano* **2011**, *5*, 3923−3929.
(46) Guan, C.-Z.; Wang, D.; Wan, L.-J. *Chem. Commun.* **2012**, *48*, 2943−2945.
(47) Kissel, P.; Erni, R.; Schweizer, W. B.; Rossell, M. D.; King, B. T.; Bauer, T.; Götzinger, S.; Schlüter, A. D.; Sakamoto, J. *Nat. Chem.* **2012**, *4*, 287−291.
(48) Spitler, E. L.; Dichtel, W. R. *Nat. Chem.* **2010**, *2*, 672−677.
(49) Biswal, B. P.; Chandra, S.; Kandambeth, S.; Lukose, B.; Heine, T.; Banerjee, R. *J. Am. Chem. Soc.* **2013**, *135*, 5328−5331.
(50) Côté, A. P.; Benin, A. I.; Ockwig, N. W.; O'Keeffe, M.; Matzger, A. J.; Yaghi, O. M. *Science* **2005**, *310*, 1166−1170.
(51) Cardenas, L.; Gutzler, R.; Lipton-Duffin, J.; Fu, C.; Brusso, J. L.; Dinca, L. E.; Vondráček, M.; Fagot-Revurat, Y.; Malterre, D.; Rosei, F.; Perepichka, D. F. *Chem. Sci.* **2013**, *4*, 3263−3268.
(52) Frisch, M. J.; et al. *Gaussian 09*, revision B.01; Gaussian, Inc.: Wallingford, CT, 2009.
(53) Nonplanar conformations are also energetically more favorable for 1D polymers **2.1** and **5.1**.
(54) Xiao, H.; Tahir-Kheli, J.; Goddard, W. A., III. *J. Phys. Chem. Lett.* **2011**, *2*, 212−217.
(55) Novoselov, K. S.; Jiang, D.; Schedin, F.; Booth, T. J.; Khotkevich, V. V.; Morozov, S. V.; Geim, A. K. *Proc. Natl. Acad. Sci. U.S.A.* **2005**, *102*, 10451−10453.
(56) Yan, X.; Li, B.; Li, L.-S. *Acc. Chem. Res.* **2012**, DOI: 10.1021/ar300137p.
(57) Müllen, K.; Rabe, J. P. *Acc. Chem. Res.* **2008**, *41*, 511−520.
(58) Blunt, M. O.; Russell, J. C.; Champness, N. R.; Beton, P. H. *Chem. Commun.* **2010**, *46*, 7157−7159.
(59) Schlütter, F.; Rossel, F.; Kivala, M.; Enkelmann, V.; Gisselbrecht, J.-P.; Ruffieux, P.; Fasel, R.; Müllen, K. *J. Am. Chem. Soc.* **2013**, *135*, 4550−4557.
(60) Lafferentz, L.; Eberhardt, V.; Dri, C.; Africh, C.; Comelli, G.; Esch, F.; Hecht, S.; Grill, L. *Nat. Chem.* **2012**, *4*, 215−220.
(61) Krasnikov, S. A.; Doyle, C. M.; Sergeeva, N. N.; Preobrajenski, A. B.; Vinogradov, N. A.; Sergeeva, Y. N.; Zakharov, A. A.; Senge, M. O.; Cafolla, A. A. *Nano Res.* **2011**, *4*, 376−384.
(62) Grimsdale, A. C.; Chan, K. L.; Martin, R. E.; Jokisz, P. G.; Holmes, A. B. *Chem. Rev.* **2009**, *109*, 897−1091.
(63) Dawson, R.; Su, F.; Niu, H.; Wood, C. D.; Jones, J. T. A.; Khimyak, Y. Z.; Cooper, A. I. *Macromolecules* **2008**, *41*, 1591−1593.
(64) Gao, X.; Zhou, Z.; Zhao, Y.; Nagase, S.; Zhang, S. B.; Chen, Z. *J. Phys. Chem. C* **2008**, *112*, 12677−12682.
(65) Hutchison, G. R.; Zhao, Y.-J.; Delley, B.; Freeman, A. J.; Ratner, M. A.; Marks, T. J. *Phys. Rev. B* **2003**, *68*, 35204.
(66) Hong, S. Y.; Kim, D. Y.; Kim, C. Y.; Hoffmann, R. *Macromolecules* **2001**, *34*, 6474−6481.
(67) Musfeldt, J. L.; Reynolds, J. R.; Tanner, D. B.; Ruiz, J. P.; Wang, J.; Pomerantz, M. *J. Polym. Sci., B: Polym. Phys.* **1994**, *32*, 2395−2404.
(68) Nguyen, M.-T.; Pignedoli, C. A.; Passerone, D. *Phys. Chem. Chem. Phys.* **2011**, *13*, 154−160.
(69) Zade, S. S.; Bendikov, M. *Chem.—Eur. J.* **2007**, *13*, 3688−3700.
(70) Shirota, Y.; Kageyama, H. *Chem. Rev.* **2007**, *107*, 953−1010.
(71) Zhou, J.; Sun, Q. *J. Am. Chem. Soc.* **2011**, *133*, 15113−15119.